

## SEARCH FOR LOW-ENERGY NEUTRINOS FROM GALACTIC GAMMA-RAY SOURCES

Y. FUKUDA, T. HAYAKAWA, K. INOUE, T. ISHIDA, T. KAJITA, Y. KOSHIO, M. NAKAHATA,  
 K. NAKAMURA, A. SAKAI, M. SHIOZAWA, J. SUZUKI, Y. SUZUKI, AND Y. TOTSUKA

Institute for Cosmic Ray Research, University of Tokyo, Tanashi, Tokyo 188, Japan

M. MORI,<sup>1</sup> K. S. HIRATA, K. KIHARA, Y. OYAMA, A. SUZUKI,<sup>2</sup> AND M. YAMADA<sup>3</sup>

National Laboratory for High Energy Physics (KEK), Tsukuba, Ibaraki 305, Japan

M. KOSHIBA AND K. NISHIJIMA

Tokai University, Shibuya, Tokyo 151, Japan

T. KAJIMURA,<sup>4</sup> T. SUDA,<sup>5</sup> AND A. T. SUZUKI

Department of Physics, Kobe University, Kobe, Hyogo 657, Japan

H. TAKEI,<sup>6</sup> K. KOGA, K. MIYANO, AND H. MIYATA

Niigata University, Niigata 950-21, Japan

T. HARA, N. KISHI, Y. NAGASHIMA, M. TAKITA, AND A. YOSHIMOTO<sup>7</sup>

Department of Physics, Osaka University, Toyonaka, Osaka 560, Japan

K. KANEYUKI, Y. TAKEUCHI, AND T. TANIMORI

Department of Physics, Tokyo Institute of Technology, Meguro-ku, Tokyo 152, Japan

S. TASAKA

Department of Physics, Gifu University, Gifu, Gifu 501-11, Japan

K. NISHIKAWA

Institute for Nuclear Study, University of Tokyo, Tanashi, Tokyo, 188, Japan

AND

E. W. BEIER, E. D. FRANK, W. FRATI, S. B. KIM,<sup>8</sup> A. K. MANN, F. M. NEWCOMER,

R. VAN BERG, AND W. ZHANG<sup>9</sup>

Department of Physics, University of Pennsylvania, Philadelphia, PA 19104

Received 1993 December 16; accepted 1994 May 3

### ABSTRACT

Data from the Kamiokande detector are used to set upper limits on fluxes of low-energy neutrinos from possible nearby sources within or near our Galaxy. The search was conducted for 1557 live detector days from 1987 January to 1993 February.

*Subject headings:* elementary particles — gamma rays: observations

### 1. INTRODUCTION

Since the publication of the directional observation in real-time of neutrinos from the Sun by the Kamiokande II collaboration (Hirata et al. 1991), questions relating to searches for other stellar sources of low-energy ( $\lesssim 30$  MeV) neutrinos have been asked of us. The Sun is  $\sim 10^5$  times closer to Earth than the next nearest stellar objects, and consequently a more distant source is required to exhibit extraordinary intensity if a neutrino signal from it is to be observed. Nevertheless, it may be useful to report the results of one such search, as we do here, to illustrate the generality of the method on which the Kamio-

kande II and III solar neutrino measurement is based, and because discoveries of very bright nearby objects (at least at certain electromagnetic wavelengths) continue to be made, e.g., PSR J0437–4715 (Johnston et al. 1993).

### 2. KAMIOKANDE DETECTOR

The Kamiokande detector is located 1000 m underground (2700 meter water equivalent) in Gifu Prefecture in western Japan. The detector is a cylindrical (14.4 m diameter, 13.1 m height) imaging water Cherenkov detector containing 2.14 metric kilotons of purified water, viewed by 948 (50 cm diameter) photomultiplier tubes (PMT) covering 20% of the detector inner surface area. An optically separated  $4\pi$  solid-angle water Cherenkov counter surrounds the detector and serves as both a passive and active shield against background events.

The Kamiokande II solar neutrino observation was started in 1987 January and extended to 1990 April, with 1040 detector live days. Further details of the Kamiokande II detector are found in Hirata et al. (1991, 1988). The new phase of the experiment, Kamiokande III, was started in 1990 December, after replacement of the entire electronics, replacement of the dead PMTs, and installation of a reflecting cone on each PMT. The

<sup>1</sup> Now at Department of Physics, Miyagi University of Education, Sendai 980, Japan.

<sup>2</sup> Now at Bubble Chamber Physics Laboratory, Tohoku University, Sendai 980, Japan.

<sup>3</sup> Now at Niigata Polytechnic College, Niigata, Japan.

<sup>4</sup> Now at Hydrographic Department, Maritime Safety Agency, Chuô-ku, Tokyo 104, Japan.

<sup>5</sup> Deceased.

<sup>6</sup> Now at Oarai Engineering Center, Power Reactor and Nuclear Fuel Development Corporation, Oarai, Ibaraki 311-13, Japan.

<sup>7</sup> Now at Public Systems Development Division, NEC Corporation, Minato-ku, Tokyo 105, Japan.

<sup>8</sup> Now at the University of Michigan, Ann Arbor, MI 48109.

<sup>9</sup> Now at NASA, Goddard Space Flight Center, Greenbelt, MD 20771.

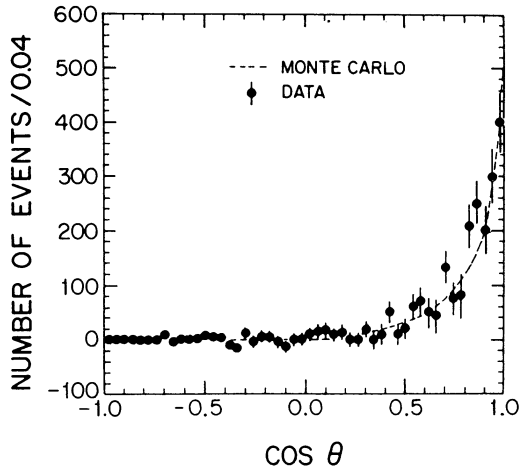


FIG. 1.—Measured and calculated electron angular distribution produced by a collimated 9 MeV  $\gamma$ -ray source (Ni-Cf) in Kamiokande II from Hirata et al. (1991).

description of the Kamiokande III detector is found in Nakamura (1993) and Inoue (1993).

Low-energy neutrinos are detected by their elastic scattering off atomic electrons. The Cherenkov radiation from the recoiling electrons is observed by the PMT. For 10 MeV electrons typically, knowing the position of the individual PMT and using their 7 ns (rms) timing resolution, we can locate the vertex of a neutrino-electron interaction to  $1.0 \sim 1.2$  m (rms), and the direction of the electron relative to the nominal incident neutrino direction can be determined to  $27^\circ$  (rms), which is set principally by multiple Coulomb scattering. (In the absence of Coulomb interactions,  $\theta_{e,\nu}^2 \leq 2m_e/E_e$ .) To illustrate the angular resolution, a comparison is shown in Figure 1 of data obtained with a collimated 9 MeV calibration  $\gamma$ -ray source with a Monte Carlo simulation of the electron angular

distribution produced by that source (Ni-Cf). Note that in searching for a signal from the Sun, the real-time observation of each electron is necessary to specify the radius vector from the Sun to the detector for comparison with the observed electron direction. The detector electron energy resolution is  $\sigma(E_e) = 0.63[E_e(\text{MeV})]^{1/2}$  and, for example, a 10 MeV electron illuminates  $\approx 30$  PMT in Kamiokande II and  $\approx 40$  PMT in Kamiokande III.

### 3. DATA REDUCTION AND ANALYSIS

The vast majority of events observed in the detector arise from radioactivity in the detector water and the rock surrounding the detector and from the inelastic interactions of cosmic-ray muons in and nearby the detector. The number of these background events is reduced by the energy, spatial, and timing criteria used to select the final sample of events. The event selection criteria are the same as those in the solar neutrino analysis described in Hirata et al. (1991), except for a few unimportant differences in the reduction of the Kamiokande III data.

In the present analysis, the threshold for the electron energy was taken to be 8 MeV and the final event samples from Kamiokande II and III were combined and binned in intervals of  $\Delta(\cos \theta_{e,\text{source}}) = 0.05$ , where  $\theta_{e,\text{source}}$  is the electron angle relative to the direction of the Sun and each of several bright sources in the Galaxy, the Galactic Center, and LMC-X4.

To investigate the angular distribution with respect to bright sources other than the Sun, the solar neutrino signal becomes part of the “background” which exhibits an angular shape peculiar to the celestial position relative to the ecliptic, and symmetric with respect to  $\theta_{e,\text{source}} = 90^\circ$ , if the data are accumulated throughout a year. Figure 2 shows the angular distribution with respect to each studied bright source of the Monte Carlo-generated solar neutrino events, where the energy threshold for electrons and live detector days are prop-

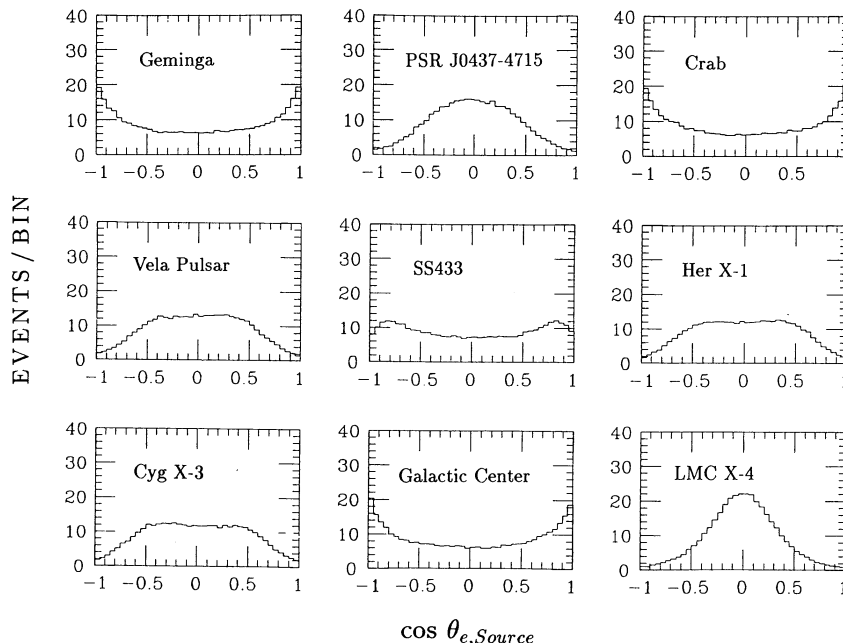


FIG. 2.—The angular distributions of the Monte Carlo-generated solar neutrino events with respect to the directions from various bright sources to Earth. These Monte Carlo events correspond to the data shown in Fig. 3j; i.e., the energy threshold for electrons (8 MeV) and live detector days are properly taken into account.

erly taken into account. For a point source located close to the ecliptic, the Sun lines up with that source twice a year, and, consequently, the angular distribution of the solar neutrinos with respect to that source peaks toward  $0^\circ$  and  $180^\circ$ . On the other hand, for a source located far from the ecliptic, the directions of the source and the Sun approximately make a right angle. Consequently, the solar-neutrino distribution peaks at  $90^\circ$  with respect to the source.

The angular distribution with respect to a point source at a fixed celestial position is, therefore, represented by an isotropic background component  $B$  and a solar-neutrino background component  $B_S$ , on which is superposed a signal of strength  $S$  from a point source. The component  $B_S$  is shown in Figure 2.

The signal  $S$  will be detected regardless of the time structure, provided that the time-integrated flux over the observation period is significantly higher than its statistical fluctuation. For the burstlike emission of low-energy neutrinos, however, a method to search for event clusters in time (Hirata et al. 1988, 1992) has a higher sensitivity. Indeed, the neutrino burst from SN 1987A, which was comprised of 11 events with only one or two being directionally correlated with the progenitor (Hirata et al. 1988), has a statistical significance of much less than  $1\sigma$  in the present analysis, as can be inferred from the results for the nine bright sources later presented in Table 1. The present analysis, on the other hand, is best suited for the search of steady or very slowly changing neutrino sources.

Since we do not know the energy spectrum of possible low-energy neutrinos from these bright sources, our basic approach is to determine  $S$  assuming monochromatic electron-neutrinos of energy  $E_\nu$ , and then to study the  $E_\nu$ -dependence of  $S$ . For this purpose, the angular distribution of the expected signal is determined for  $E_\nu = 10, 12, 14,$  and  $15$  MeV using Monte Carlo-generated events. Electron-antineutrinos, muon- and tau-neutrinos, and muon- and tau-antineutrinos are not considered, but the result for electron neutrinos only can be easily converted to the result for a given flux ratio of  $\nu_e:\bar{\nu}_e:\nu_\mu:\bar{\nu}_\mu:\nu_\tau:\bar{\nu}_\tau$  at each  $E_\nu$  using the known cross section ratios at the relevant energies of  $\sigma(\nu_e e \rightarrow \nu_e e):\sigma(\bar{\nu}_e e \rightarrow \bar{\nu}_e e) \approx 2.5:1$ ,  $\sigma(\nu_e e \rightarrow \nu_e e):\sigma(\nu_{\mu,\tau} e \rightarrow \nu_{\mu,\tau} e) \approx 6:1$ , and  $\sigma(\nu_e e \rightarrow \nu_e e):\sigma(\bar{\nu}_{\mu,\tau} e \rightarrow \bar{\nu}_{\mu,\tau} e) \approx 7:1$  because the signal angular distribution is mainly determined by the angular resolution. Here, it is assumed

that the reaction  $\bar{\nu}_e p \rightarrow e^+ n$  gives an isotropic angular distribution which is indistinguishable from the background.

#### 4. RESULTS AND DISCUSSION

For the studied bright point sources other than the Sun, the quantities  $B$  and  $S$  are determined using a maximum-likelihood method from the best fits of the assumed angular distribution to the data. The numerical results for  $E_\nu = 10$  MeV are given in Table 1. Figures 3a–3i show the resulting angular distributions with the solar-neutrino component  $B_S$  subtracted. The overlaid dashed lines show the numerical results for  $E_\nu = 10$  MeV. The 90% confidence-level  $\nu_e$  flux upper limits given in column (6) of Table 1 were calculated from the respective likelihood function by limiting the domain of the variable  $S$  to be the physical region,  $S \geq 0$ . The  $E_\nu$ -dependence of the results is graphically summarized in Figure 4.

For comparison, Figure 3j shows the angular distribution with respect to the Sun for  $E_e \geq 8$  MeV. The solid line shows the result of a maximum-likelihood analysis. For the case of the Sun, as was described in Hirata et al. (1991), it was assumed that the distribution is represented by an isotropic component due to the background  $B$  on which is superposed a signal of strength  $S$  from the Sun. The expected electron angular distribution is obtained by integrating above the analysis threshold the product of the  ${}^8\text{B}$  solar neutrino energy spectrum and the energy-dependent elastic scattering cross section. In Table 1 the numerical result for the Sun with  $E_e \geq 8$  MeV is also given. As expected, the Sun is the only source exhibiting a statistically significant signal.

#### 5. CONCLUSIONS

The upper limits on neutrino fluxes from different directions in the sky given in column (6) of Table 1, and indicated by right ascensions and declinations in columns (2) and (3), are of some intrinsic interest. For example, the upper limit on the recently discovered pulsar PSR J0437–4715, a very bright nearby binary pulsar with a low-mass companion (Johnston et al. 1993), indicates that significant steady or rapidly pulsed emission of low-energy neutrinos does not occur from that relatively bright source of electromagnetic radiation.

TABLE 1  
SUMMARY OF UPPER LIMITS ON ELECTRON-NEUTRINO FLUXES AT  $E_\nu = 10$  MeV INCIDENT ON  
EARTH FROM THE INDICATED SOURCES OTHER THAN THE SUN

Source (1)	R.A. (2)	Decl. (3)	Distance (kpc) (4)	Events (5)	90% C.L. $\nu_e$ flux Upper Limit ( $\text{cm}^{-2} \text{s}^{-1}$ ) (6)	90% C.L. $\nu_e$ Luminosity Upper Limit ( $\text{ergs s}^{-1}$ ) (7)
Geminga .....	97:7	17:8	0.1 <sup>a</sup>	$-1^{+22}_{-21}$	$1.0 \times 10^5$	$1.9 \times 10^{42}$
PSR J0437–4715 .....	69.32	–47.25	0.15	$-12^{+20}_{-19}$	$8.0 \times 10^4$	$3.4 \times 10^{42}$
Crab .....	82.9	22.0	2	$-17^{+22}_{-20}$	$7.9 \times 10^4$	$6.1 \times 10^{44}$
Vela Pulsar .....	128.4	–45	0.5	$-4^{+20}_{-18}$	$9.7 \times 10^4$	$4.6 \times 10^{43}$
SS 433 .....	285.1	4.8	3	$-25^{+19}_{-17}$	$6.0 \times 10^4$	$1.0 \times 10^{45}$
Her X-1 .....	254.0	35.4	5	$2^{+21}_{-19}$	$1.0 \times 10^5$	$4.8 \times 10^{45}$
Cyg X-3 .....	307.6	40.8	12	$20^{+21}_{-19}$	$1.4 \times 10^5$	$3.9 \times 10^{46}$
Galactic Center .....	265.5	–28.6	10	$-40^{+19}_{-17}$	$4.9 \times 10^4$	$9.4 \times 10^{45}$
LMC X-4 .....	81.0	–69.5	50	$-23^{+19}_{-18}$	$6.4 \times 10^4$	$3.1 \times 10^{47}$
Sun .....	...	...	$5 \times 10^{-9}$	$358^{+29}_{-28}$ <sup>b</sup>	...	...

<sup>a</sup> See Bignami, Caraveo, & Mereghetti 1993.

<sup>b</sup> The  ${}^8\text{B}$  solar neutrino flux obtained from this result is statistically consistent with the published result by Kamiokande II (Hirata et al. 1991),  $0.46 \pm 0.05$  (stat.)  $\pm 0.06$  (syst.) times the standard solar model prediction (Bahcall & Ulrich 1988).

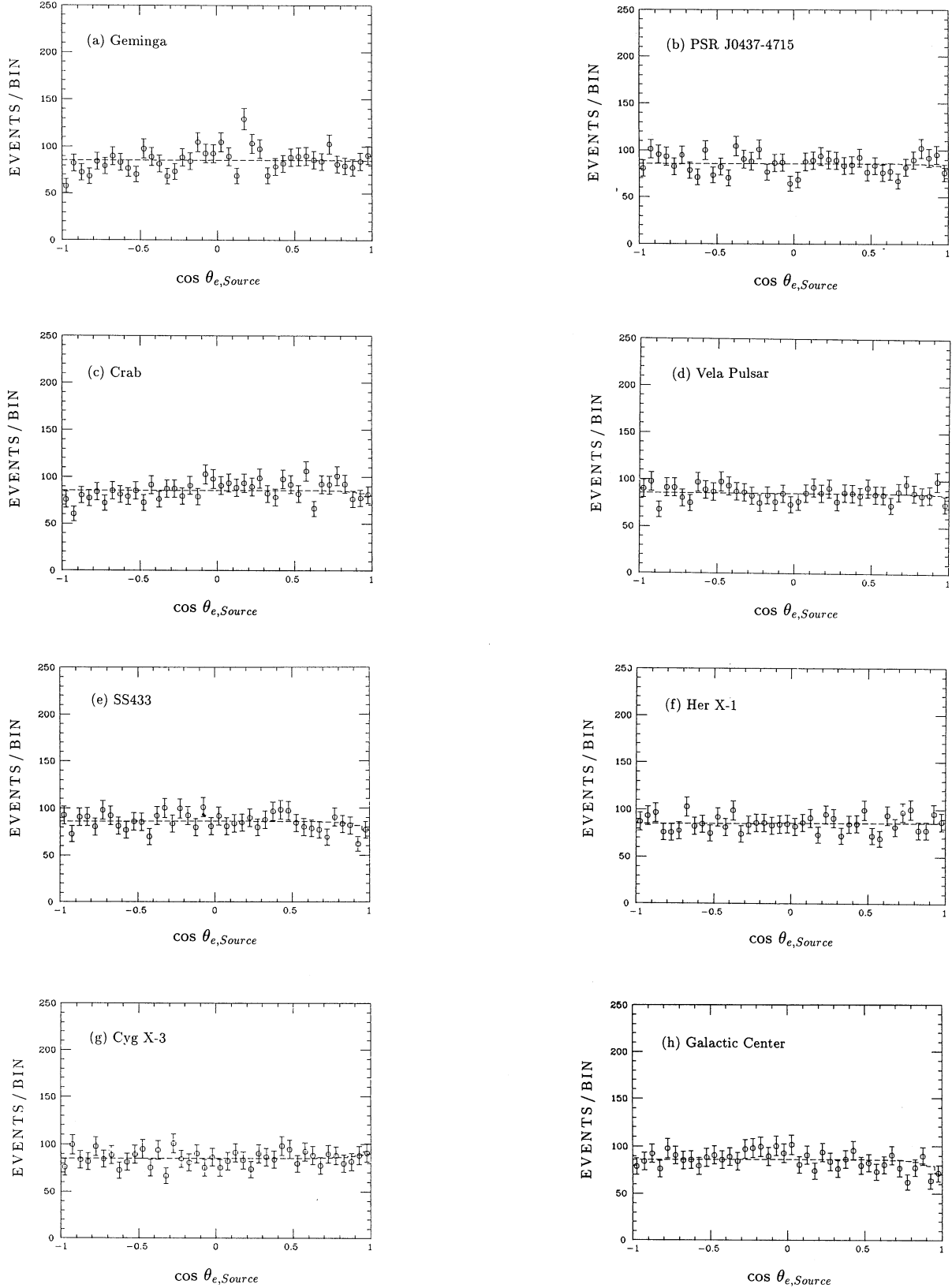


FIG. 3.—(a)–(i) The data points indicated by the circles show the angular distributions from which the fitted solar-neutrino component is subtracted. The numerical results indicated by the dashed lines correspond to a superposition of a flat background and a possible source signal for monochromatic electron-neutrinos of  $E_\nu = 10$  MeV. (j) The electron angular distribution for  $E_e \geq 8$  MeV (combined data from Kamiokande II and III) with respect to the direction from the Sun to Earth. The solid line is the best fit to a flat background plus a  ${}^8\text{B}$  solar-neutrino signal.

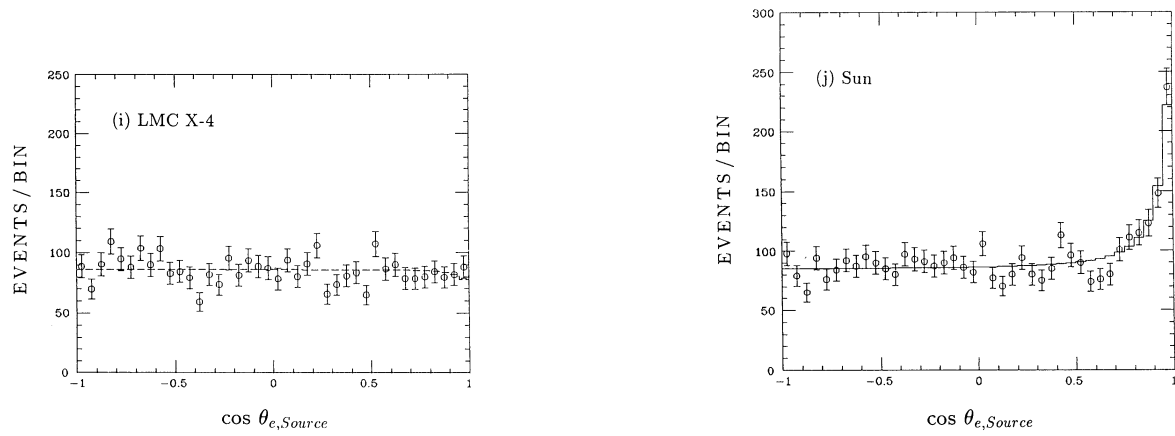


FIG. 3—Continued

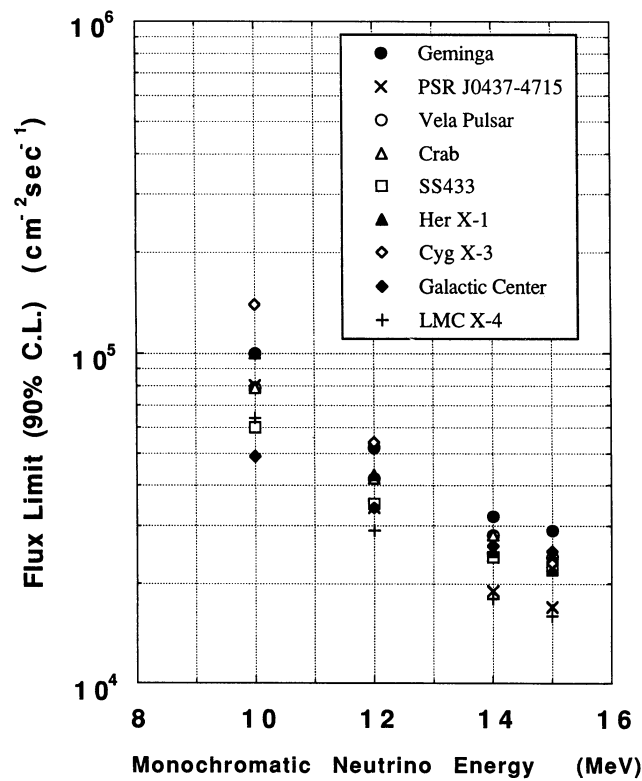


FIG. 4.—Summary of the 90% confidence level upper limits of the  $\nu_e$  flux incident on Earth from the directions of the various indicated sources, as a function of assumed monochromatic neutrino energy  $E_\nu$ .

## REFERENCES

- Bahcall, J. N., & Ulrich, R. K. 1988, *Rev. Mod. Phys.*, 60, 297  
 Bignami, G. F., Caraveo, P. A., & Mereghetti, S. 1993, *Nature*, 361, 704  
 Hirata, K. S., et al. 1988, *Phys. Rev. D*, 38, 448  
 ———. 1991, *Phys. Rev. D*, 44, 2241  
 ———. 1992, *Phys. Rev. D*, 45, 3355

- Inoue, K. 1993, in *Electroweak Interactions and Unified Theories*, ed. J. Trần Thanh Vân (Gif-sur Yvette: Editions Frontières), 385  
 Johnston, S., et al. 1993, *Nature*, 361, 613  
 Nakamura, K. 1993, *Nucl. Phys. B (Proc. Suppl.)*, 31, 105